

# Thyroid hormone receptors promote metastasis of human hepatoma cells via regulation of *TRAIL*

H-C Chi<sup>1</sup>, S-L Chen<sup>2</sup>, C-J Liao<sup>1</sup>, C-H Liao<sup>1</sup>, M-M Tsai<sup>1,3</sup>, Y-H Lin<sup>1</sup>, Y-H Huang<sup>4</sup>, C-T Yeh<sup>5</sup>, S-M Wu<sup>1</sup>, Y-H Tseng<sup>1</sup>, C-Y Chen<sup>1</sup>, C-Y Tsai<sup>1</sup>, I-H Chung<sup>1</sup>, W-J Chen<sup>6</sup> and K-H Lin<sup>\*1</sup>

Although accumulating evidence has confirmed the important roles of thyroid hormone ( $T_3$ ) and its receptors (TRs) in tumor progression, the specific functions of TRs in carcinogenesis remain unclear. In the present study, tumor necrosis factor (TNF)-related apoptosis-inducing ligand (*TRAIL*) was directly upregulated by  $T_3$  in TR-overexpressing hepatoma cell lines. *TRAIL* is an apoptotic inducer, but it can nonetheless trigger non-apoptotic signals favoring tumorigenesis in apoptosis-resistant cancer cells. We found that TR-overexpressing hepatoma cells treated with  $T_3$  were apoptosis resistant, even when *TRAIL* was upregulated. This apoptotic resistance may be attributable to simultaneous upregulation of *Bcl-xL* by  $T_3$ , because (1) knockdown of  $T_3$ -induced *Bcl-xL* expression suppressed  $T_3$ -mediated protection against apoptosis, and (2) overexpression of *Bcl-xL* further protected hepatoma cells from *TRAIL*-induced apoptotic death, consequently leading to *TRAIL*-promoted metastasis of hepatoma cells. Moreover,  $T_3$ -enhanced metastasis *in vivo* was repressed by the treatment of *TRAIL*-blocking antibody. Notably, *TRAIL* was highly expressed in a subset of hepatocellular carcinoma (HCC) patients, and this high-level expression was significantly correlated with that of TRs in these HCC tissues. Together, our findings provide evidence for the existence of a novel mechanistic link between increased TR and *TRAIL* levels in HCC. Thus, TRs induce *TRAIL* expression, and *TRAIL* thus synthesized acts in concert with simultaneously synthesized *Bcl-xL* to promote metastasis, but not apoptosis.

*Cell Death and Differentiation* (2012) 19, 1802–1814; doi:10.1038/cdd.2012.58; published online 11 May 2012

The thyroid hormone 3,3',5-tri-iodo-L-thyronine ( $T_3$ ) is a significant regulator of genes that function in cell development, differentiation, growth, and other aspects of metabolism. The actions of  $T_3$  are mediated by nuclear thyroid hormone receptors (TRs); these are ligand-dependent transcription factors encoded by two genes, *TR $\alpha$*  and *TR $\beta$* . TRs contain functional modular domains involved in ligand and DNA binding, homo- and hetero-dimerization with other receptors, and interaction with other transcription factors or co-factors. Binding of a ligand triggers conformational changes in TRs which, in turn, stimulate release of co-repressors and recruitment of transcriptional co-activators to enhance target gene transcription.<sup>1</sup>

Accumulating evidence from recent studies supports the existence of an association between aberrant TR regulation (or *TR* mutation) and human neoplasia.<sup>2</sup> However, any specific role played by TRs in tumorigenesis remains unclear. Notably, a mutant form of TR (*v-erbA*) that has lost ligand-binding ability causes development of hepatocellular carcinoma (HCC) in transgenic mice.<sup>3,4</sup> Moreover, earlier experiments by our group and others showed that cDNAs

encoding *TR $\alpha$*  and *TR $\beta$*  were truncated, or mutated at high frequencies, in human HCCs.<sup>5–7</sup> A few studies have implicated  $T_3$  as a potential tumor inducer in several types of cancer.<sup>8–10</sup> For example,  $T_3$  and TRs promoted intestinal cell proliferation and tumorigenesis, by interaction with the Wnt pathway, and also induced the synthesis of  $\beta$ -catenin and some of its target genes.<sup>11</sup> Additionally, hyperthyroxinemia has been reported to increase the frequency of colon cancer development in a rat experimental model.<sup>12</sup>

We used a cDNA microarray to identify genes upregulated by  $T_3$  in a *TR $\alpha$* -overexpressing hepatoma cell line (HepG2-*TR $\alpha$* 1); we sought to elucidate the role played by  $T_3$ /TRs in human hepatocellular carcinogenesis. Tumor necrosis factor (TNF)-related apoptosis-inducing ligand (*TRAIL*/Apo2L), a potent effector of tumorigenesis, was the focus of our further study.

*TRAIL* was cloned on the basis of gene homology with DNA encoding the extracellular domain of TNF and the CD95 ligand (FASL).<sup>13,14</sup> As with other members of the TNF family, human *TRAIL* is a type II transmembrane protein containing 281 amino-acid residues. Cleavage of the C-terminal region

<sup>1</sup>Department of Biochemistry, School of Medicine, Chang-Gung University, Taoyuan, Taiwan; <sup>2</sup>Department of Life Sciences, National Central University, Zhongli, Taiwan; <sup>3</sup>Department of Nursing, Chang-Gung University of Science and Technology, Taoyuan, Taiwan; <sup>4</sup>Medical Research Central, Chang Gung Memorial Hospital, Taoyuan, Taiwan; <sup>5</sup>Liver Research Unit, Chang-Gung Medical Center, Taipei, Taiwan and <sup>6</sup>First Cardiovascular Division, Chang Gung Memorial Hospital, Taoyuan, Taiwan

\*Corresponding author: K-H Lin, Department of Biochemistry, School of Medicine, Chang-Gung University, 259 Wen-hwa 1 Road, Taoyuan 333, Taiwan. Tel/Fax: + 886 3211 8263; E-mail: khlin@mail.cgu.edu.tw

**Keywords:** thyroid hormone receptor; *TRAIL*; apoptosis; metastasis

**Abbreviations:**  $T_3$ , thyroid hormone; TRs, thyroid hormone receptors; TRE, thyroid response element; *TRAIL*, TNF-related apoptosis-inducing ligand; HCC, hepatocellular carcinoma; ActD, actinomycin D; CHX, cycloheximide; (r)-*TRAIL*, recombinant *TRAIL*; Ad-*TRAIL*, Adenovirus expressing *TRAIL*; NF- $\kappa$ B, nuclear factor kappa B; cFLIP, cellular FLICE-like inhibitory protein; MAPK, mitogen-activated protein kinase; PKC, protein kinase C; MMP, matrix metalloproteinase; SCID, severe combined immunodeficiency; H&E, hematoxylin and eosin; IHC, immunohistochemical staining; ChIP, chromatin immunoprecipitation

Received 14.10.11; revised 28.2.12; accepted 02.4.12; Edited by JP Medema; published online 11.5.12

(the extracellular domain) by a cysteine protease releases a soluble form of TRAIL. Both the soluble and membrane-bound forms of TRAIL are functionally active. Most investigations to date have focused on the ability of TRAIL to induce apoptosis in cancer cells. However, a few studies have additionally shown that TRAIL not only promotes apoptosis but also triggers non-apoptotic pathways, including those involving the activities of protein kinase C, nuclear factor kappa B (NF- $\kappa$ B), and mitogen-activated protein kinases (MAPK).<sup>15</sup> The non-apoptotic signaling pathways stimulated by TRAIL induce genes that promote cell survival, angiogenesis, and metastasis, and that contribute to cancer progression.

Thus, TRAIL may be a potential candidate for cancer therapy. However, TRAIL also promotes tumor progression. In apoptosis-resistant cancer cells, TRAIL facilitates tumor progression by promoting cell migration and invasion.<sup>16–20</sup> Consistent with these findings, earlier studies showed that TRAIL was abnormally expressed in several human cancers, especially tumors of advanced grade, including non-small cell lung cancer, pancreatic cancer, colorectal cancer, and cholangiocarcinoma.<sup>20–22</sup> However, these observations are inconsistent with the notion that TRAIL serves as a tumor killer, rather implying that the role of TRAIL in tumorigenesis depends on whether cells are or not resistant to TRAIL. Bcl-xL has been reported to suppress TRAIL-mediated apoptosis in several cell types.<sup>16,23</sup>

In the current work, we showed that T<sub>3</sub> upregulated *TRAIL* expression at the transcriptional level in TR-overexpressing hepatoma cells. Further, we identified a thyroid response element (TRE) in the *TRAIL* promoter. Notably, expression of T<sub>3</sub>-induced *Bcl-xL* protected cells from death induced by simultaneous expression of TRAIL. Our findings suggest that TRAIL contributes to tumor progression by promoting cancer cell migration and invasion following T<sub>3</sub> treatment.

## Results

**T<sub>3</sub> regulates *TRAIL* mRNA and protein levels in TR-overexpressing hepatoma cells.** To explore the roles played by TRs in hepatocellular carcinogenesis, a cDNA microarray was used to identify genes regulated by T<sub>3</sub> in HepG2-TR $\alpha$  cells. One such gene, *TRAIL*, was highly upregulated 48 h after treatment with T<sub>3</sub>. Subsequently, real-time PCR was utilized to verify this finding, employing established stable cell lines, including HepG2-TR $\alpha$ #1, #2, -TR $\beta$ , and -Neo; these cells express different levels or isoforms of TRs (Figure 1a). As shown in Figure 1b, the levels of mRNA encoding *TRAIL* were enhanced in a time-, dose-, and TR-dependent manner in various TR-overexpressing cell lines after T<sub>3</sub> treatment.

The effect of T<sub>3</sub> on TRAIL protein expression was additionally assessed in several hepatoma cell lines. After treatment with (or without) T<sub>3</sub> (1 or 10 nM) for 24 or 48 h, TRAIL protein levels in culture medium and total lysates were analyzed by western blotting. Notably, both intracellular and secreted TRAIL levels were dramatically upregulated (by ~2–15-fold) by T<sub>3</sub> in HepG2-TR $\alpha$ #1, #2, -TR $\beta$ , and -Neo cell lines (Figure 1c; Supplementary Figure 1); induction of TRAIL by T<sub>3</sub> was dependent on the TR expression level in the various cell lines (Figure 1d). In other hepatoma cell lines, including J7-TR and Huh7, that express exogenous or endogenous TR proteins, T<sub>3</sub> enhanced the levels of cellular and secreted TRAIL protein, similar to that observed in HepG2-TR cells (Figure 1c; Supplementary Figure 1). Our results clearly show that T<sub>3</sub> increases *TRAIL* expression in hepatoma cells at both the mRNA and protein levels, in a TR-dependent manner.

**T<sub>3</sub> regulates *TRAIL* expression at the transcriptional level.** To elucidate the mechanism underlying T<sub>3</sub>-mediated

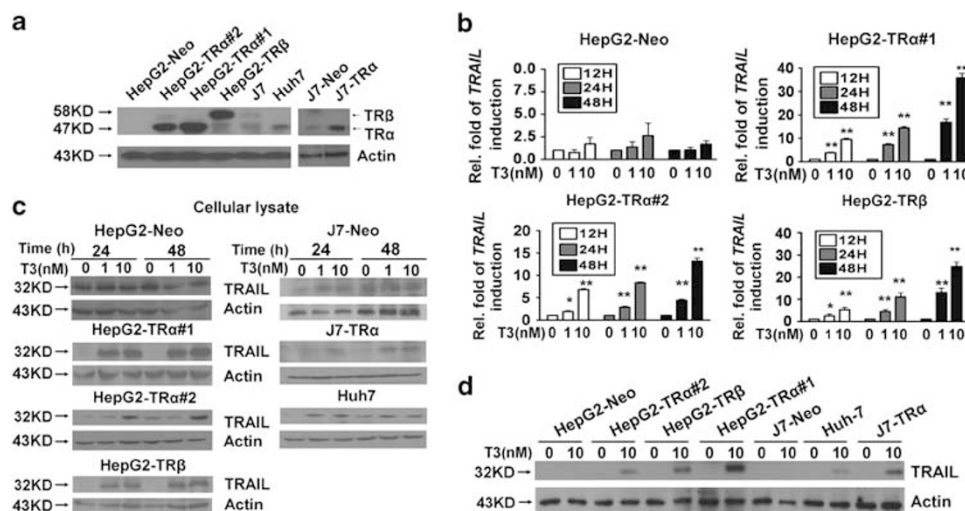


**Figure 1** Effects of T<sub>3</sub> on the levels of *TRAIL*-encoding mRNA and protein in hepatoma cell lines. (a) Detection (by western blotting) of TR proteins in HCC cell lines and TR-overexpressing or vector control (neo) stable cell lines derived from HepG2 and J7 cells. (b) Total RNA from TR-overexpressing or vector control (neo) stable cell lines maintained in T<sub>3</sub>-depleted medium (Td; (T<sub>3</sub>) = 0 nM) or T<sub>3</sub>-supplemented medium ((T<sub>3</sub>) = 1 or 10 nM) for 12, 24, or 48 h was prepared before analysis of *TRAIL* mRNA expression by real-time PCR. The *TRAIL* mRNA expression level of cells maintained in Td medium was arbitrarily set at unity; expression levels in cells treated with T<sub>3</sub> were compared with those in Td cells. The data are mean  $\pm$  S.E.M. of data derived from three independent experiments. \*\**P* < 0.01; \**P* < 0.05, with respect to levels in Td cells; Student's *t*-test. (c and d) TRAIL protein levels in total lysates (100  $\mu$ g amounts) of parental and stable HCC cell lines maintained in serum-free medium with or without T<sub>3</sub> (1 or 10 nM) for 24 or 48 h, as determined by Western blotting. To ensure T<sub>3</sub> depletion, cells were maintained in Td medium for 24 h before the addition of serum-free medium. Actin signals served as loading controls

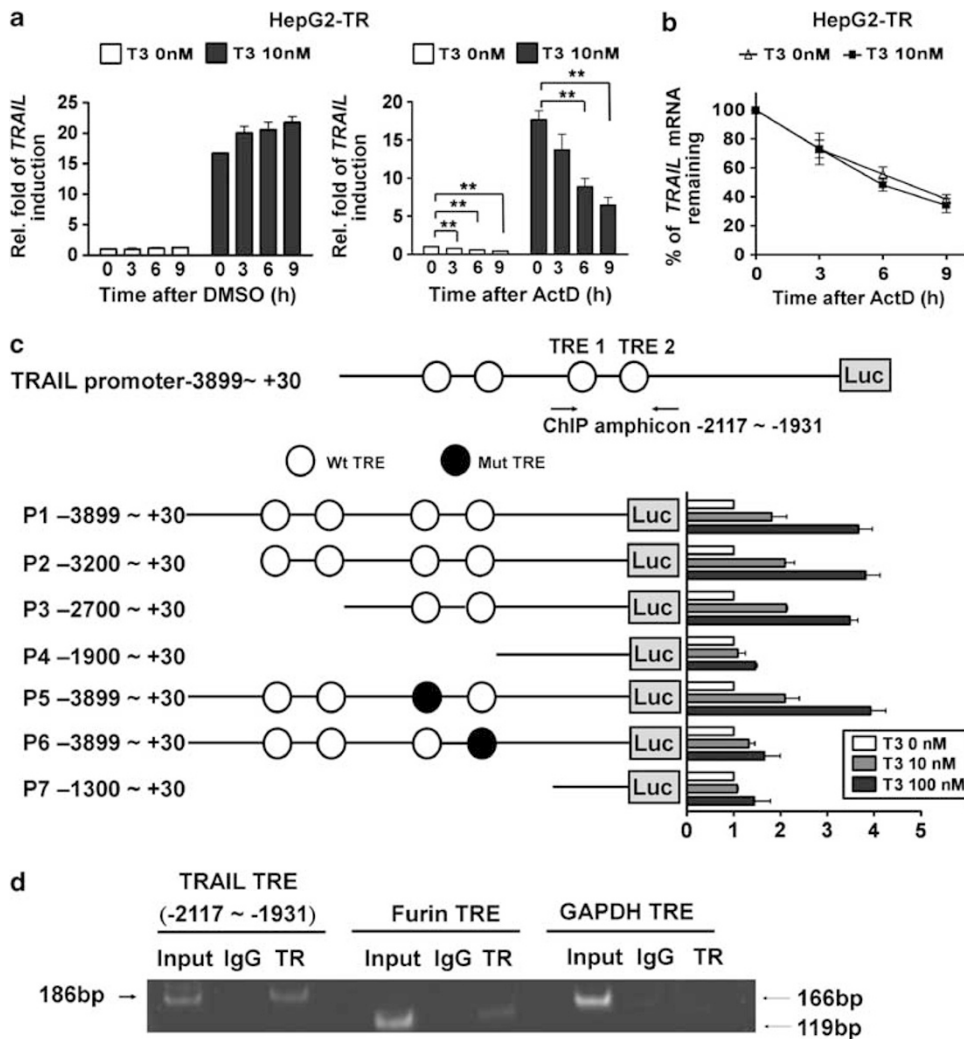


**Figure 2** Regulation of *TRAIL* expression at the transcriptional level by  $T_3$ . (a)  $T_3$  does not affect the stability of *TRAIL*-encoding mRNA. After stimulation with  $T_3$  (0 or 10 nM) for 24 h, HepG2-TR $\alpha$  cells were treated with vehicle or actinomycin D (ActD, 2  $\mu$ g/ml) for the indicated times. Total RNA was isolated and subjected to real-time PCR analysis. The level of *TRAIL* relative to that in cells harvested at the commencement of treatment (thus without exposure to  $T_3$ ) are shown. (b) The values obtained at the indicated time-points are presented as percentages of residual RNA levels relative to those present at commencement of ActD treatment. The data are mean  $\pm$  S.E.M. of values derived from the data of three independent experiments. Statistical analysis was performed using one-way ANOVA.  $**P < 0.01$ . (c) The *TRAIL* 5'-flanking region (-3899 to +30; P1), and *TRAIL* 5'-deletion and TRE mutants, were cloned into the pGL3-basic vector to generate luciferase-reporter plasmids. After co-transfection with a plasmid expressing  $\beta$ -galactosidase (to allow estimation of transfection efficiency), HepG2-TR cells were harvested following treatment with  $T_3$  (0, 10, or 100 nM) for 24 h. Luciferase activity was normalized to that of  $\beta$ -galactosidase. In addition, serial deletions within the *TRAIL* promoter region were constructed (plasmids P2-P7) and transfected into HepG2-TR cells; promoter activity analysis followed. The data are mean  $\pm$  S.E.M. of values derived from three independent experiments, each performed in triplicate. (d) TR is recruited, *in vivo*, to TREs within the *TRAIL* promoter region. Complexes of chromatin and factors bound thereto were immunoprecipitated using either control IgG or an antibody directed against TRs. Next, precipitated DNA was eluted, purified, and detected by PCR using primers targeting the TRE1 region of the *TRAIL* promoter. Signals from the *Furin* promoter and *Gapdh* gene served as positive and negative controls, respectively

enhancement of *TRAIL* expression, we examined *TRAIL* transcript stability by suppressing new mRNA synthesis by HepG2-TR and J7-TR cells with actinomycin D (ActD; 2  $\mu$ g/ml). Although ActD efficiently suppressed *TRAIL* mRNA production, even in the control cells expressed a little amount of *TRAIL* mRNA (Figure 2a; Supplementary Figure 2A), the half-life of *TRAIL* mRNA was similar in cells exposed or not exposed to  $T_3$  (Figure 2b; Supplementary Figure 2B). This indicates that induction of *TRAIL* mRNA synthesis by  $T_3$  is not accompanied by any variation in RNA stability.

To determine whether  $T_3$  activated *TRAIL* transcription, we cloned the human *TRAIL* promoter region, encompassing the

nucleotides from position -3899 to +30 (termed promoter region 1; P1), and placed this sequence upstream of the luciferase reporter gene in a pGL3-basic vector. Several putative TREs have been identified in this region.

In the presence of 100 nM  $T_3$ , the activity of our reporter construct (P1, with four predicted TREs) was increased by approximately four fold in HepG2-TR cells (Figure 2c, right panel), indicating that TRs directly target this promoter region. To identify functional TREs in the *TRAIL* promoter, a series of 5'-deletion mutants of the *TRAIL* promoter region were generated; various numbers of TREs were retained (Figure 2c, P2-P7). We found that  $T_3$  treatment enhanced

the activities of reporters containing the sequences -3200 to +30 (P2) and -2700 to +30 (P3), by up to 4- and 3.6-fold, respectively. However, the deletion mutant -1900 to +30 (P4) lost T<sub>3</sub>-induced promoter activity (Figure 2c, right panel), implying that *cis*-elements lying between -2700 and -1900 mediated the T<sub>3</sub> effect. Two putative TREs, TRE1 and TRE2 (at -2068 to -2180 and -1967 to -1977, respectively), were identified within this region and each was separately mutated to determine the precise role played by the TRE in T<sub>3</sub>-induced *TRAIL* promoter activity. Mutation of TRE1 had no effect on T<sub>3</sub>-induced *TRAIL* promoter activity. However, mutation of TRE2 significantly reduced the response of the *TRAIL* promoter to T<sub>3</sub>.

Together, these data suggest that TRE2, located between positions -1967 and -1977, mediates the effect of T<sub>3</sub> on the *TRAIL* promoter. Further analysis of the TRE2 sequence, 5'-ATCTCTTGACCT-3', revealed the existence of an atypical palindromic TRE. Targeting of TRE2 by TRs *in vivo* was further confirmed using the chromatin immunoprecipitation (ChIP) assay in HepG2-TR cells (Figure 2d). Binding of TR to the *Furin* promoter and *Gapdh* gene served as positive and negative controls, respectively.

**T<sub>3</sub> protects TR-overexpressing hepatoma cells from apoptosis.** Previous studies have suggested that *TRAIL*

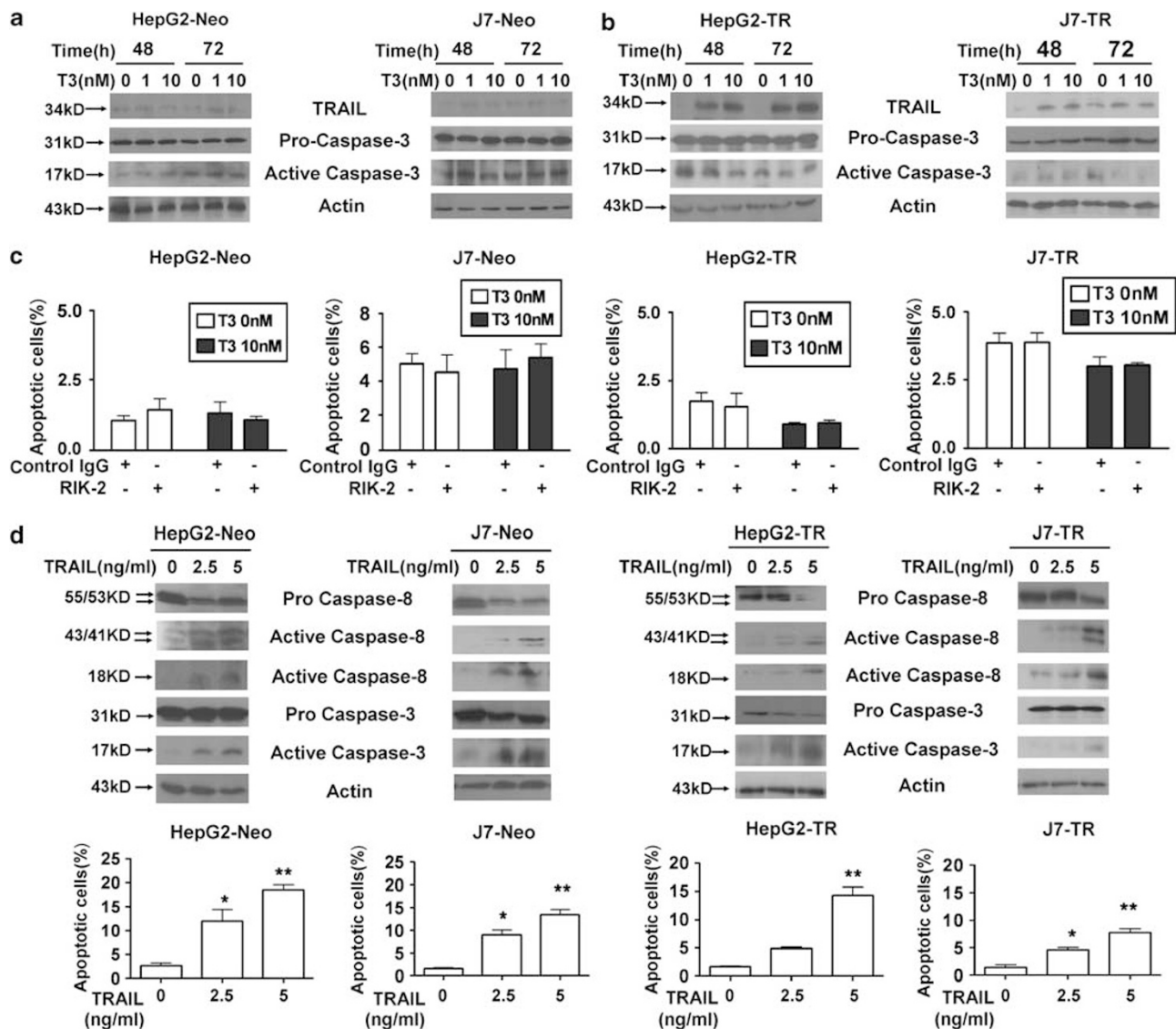


**Figure 3** T<sub>3</sub>-induced *TRAIL* synthesis does not trigger apoptosis in hepatoma cells. Control (a) and TR-overexpressing (b) HepG2 and J7 cells were cultured in T<sub>3</sub>-depleted medium with or without T<sub>3</sub> (1 or 10 nM) for 24 or 48 h before harvesting and analysis of the expression levels of *TRAIL*, and the proform and active form of caspase-3, in 100 μg lysis aliquots, by western blotting. Actin signals served as internal controls. (c) The proportions of apoptosis induced by T<sub>3</sub> in cells pretreated with control IgG or a *TRAIL*-blocking antibody (RIK-2, 10 μg/ml) were determined using flow cytometry followed by staining for PI. The data are presented as mean ± S.E.M. of those of experiments performed in triplicate. Statistical analysis employed one-way ANOVA; no significant among-treatment difference was evident for any cell line. (d) *TRAIL* induces apoptosis in control and TR-overexpressing hepatoma cells. HepG2-Neo, J7-Neo, HepG2-TR, and J7-TR cells were treated with r-*TRAIL* (2.5 or 5 ng/ml) for 48 h. After such stimulation, the extent of activation of caspase-8 and caspase-3 was analyzed by western blotting (upper panel). The proportions of apoptotic cells in the same samples were determined using flow cytometry; the results are shown in the bottom panels. All data are presented as mean ± S.E.M. of those of experiments performed in triplicate. Among-treatment differences were analyzed by one-way ANOVA. \**P* < 0.05; \*\**P* < 0.01

has a pro-apoptotic role during tumor progression. As *TRAIL* expression was positively regulated by  $T_3$  in TR-expressing hepatoma cells, it was of interest to explore whether  $T_3$  could trigger apoptosis by induction of *TRAIL* in TR-overexpressing hepatoma cells. Treatment with  $T_3$  did not promote active caspase-3 induction in control HepG2 or J7 cells (Figure 3a).

Surprisingly, similar data were obtained when  $T_3$ -treated HepG2-TR or J7-TR cells were examined, although the level of *TRAIL* expression was significantly increased following  $T_3$  stimulation (Figure 3b). Moreover, as in control HepG2 and J7 cells, the percentage of apoptotic cells and Caspase-3-like activity in TR-overexpressing cells were not affected by

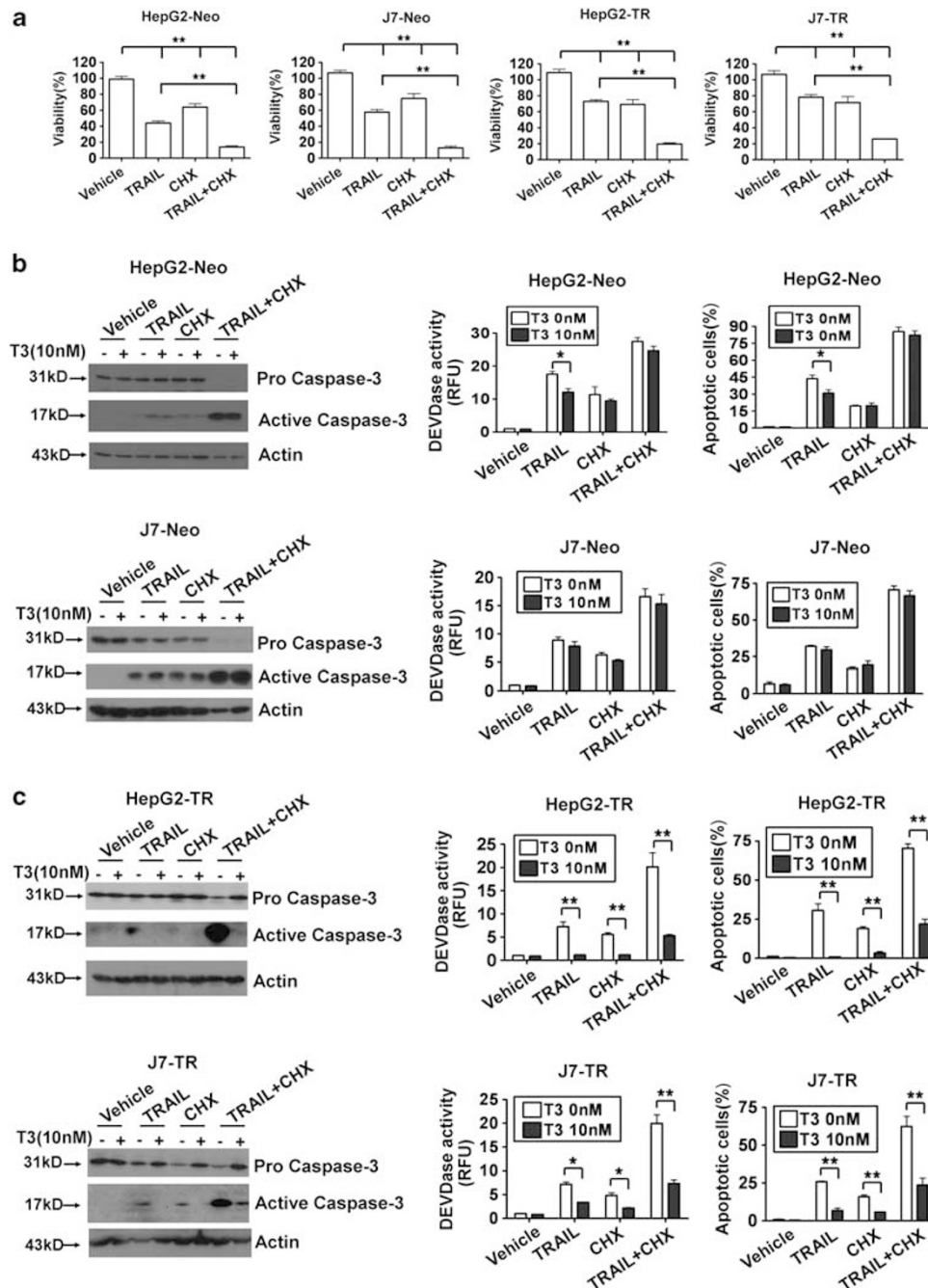


**Figure 4**  $T_3$ /TR suppresses TRAIL- and cycloheximide (CHX)-induced apoptosis. (a) The anti-tumor effects evident upon addition of r-TRAIL, CHX, and r-TRAIL plus CHX, to control or TR-overexpressing hepatoma cell lines. HepG2-Neo, J7-Neo, HepG2-TR, and J7-TR cells were treated with r-TRAIL (100 ng/ml; or not) in combination with vehicle or 2.5  $\mu$ M CHX, for 24 h. After stimulation, cell viability was measured using the MTT assay and the data are presented as relative absorbance values (in %) of control cells. (b and c)  $T_3$  protects hepatoma cells from TRAIL- or CHX-induced apoptosis. Control (b) and TR-overexpressing cells (c) were treated with the indicated reagents for 24 h after  $T_3$  (0 or 10 nM) stimulation for 2 days. Next, the extent of caspase-3 activation was determined by western blotting (left panels) and the DEVDase activity assay (middle panels). The proportions of apoptotic cells in samples subjected to various treatments were assessed using flow cytometry (right panels). Data are presented as mean  $\pm$  S.E.M. of data derived from experiments performed in triplicate; differences among treatments were analyzed using one-way ANOVA. \* $P < 0.05$ ; \*\* $P < 0.01$

$T_3$  addition, even when an effective TRAIL-neutralizing antibody, RIK-2, was added (Figure 3c, Supplementary Figures 3A-C, and 4A). These results imply that TRAIL upregulation by  $T_3$  is not associated with a significant apoptotic effect in TR-overexpressing hepatoma cells. To ascertain whether TRAIL promoted apoptotic cell death in our experimental system, control and TR-overexpressing cells were stimulated with recombinant (r)-TRAIL or were infected with adenovirus-expressing TRAIL (Ad-TRAIL). As expected, apoptotic events, as evidenced by increased activation of caspase-3/-8, and the numbers of cells in sub-G1 populations were induced following TRAIL stimulation (Figure 3d; Supplementary Figures 4b, and 5). To further clarify the relationship between  $T_3$  expression and TRAIL in terms of cell death control, r-TRAIL and several chemotherapeutic drugs, including cycloheximide (CHX), cisplatin, and etoposide that, synergistically with TRAIL, promote tumor cell apoptosis,<sup>24</sup> were added to cultures of such cells. We found that all tested drugs, used either individually or in combination, enhanced TRAIL-induced cell death (Figure 4a; Supplementary Figure 6). Surprisingly,  $T_3$  treatment of control cells only marginally suppressed the apoptosis induced by these agents (Figure 4b; Supplementary Figure 7). In contrast, apoptotic events following addition of r-TRAIL, chemotherapeutic drugs, or r-TRAIL in combination with individual drugs were significantly reduced in  $T_3$ -treated TR-overexpressing cells (Figure 4c; Supplementary Figure 8). These results suggest that  $T_3$  acts as an anti-apoptotic factor in TR-overexpressing hepatoma cells challenged with TRAIL or chemotherapeutic drugs. However, further studies were required to determine the mechanism by which  $T_3$  prevents apoptosis with simultaneous activation of the pro-apoptotic factor, TRAIL.

**$T_3$ -induced *Bcl-xL* upregulation protects hepatoma cells against TRAIL-induced apoptosis.** Although TRAIL promoted apoptosis of hepatoma cells, this effect was prevented by the addition of  $T_3$  to TR-overexpressing hepatoma cells, even after TRAIL was significantly induced. To define the mechanism employed by  $T_3$ /TRs to antagonize the apoptotic effects of TRAIL, TR target genes that may mediate this effect were further explored. Previous studies have shown that several genes exhibit an anti-apoptotic potential after TRAIL stimulation, such as NF- $\kappa$ B, the cellular FLICE-like inhibitory protein (cFLIP), and members of the Bcl-2 family (Bcl-2, Bcl-xL, Mcl-1, Bax, Bad, and Bid).<sup>25</sup> Of these factors, Bcl-xL was dramatically (~4–5-fold) enhanced upon  $T_3$  addition to HepG2-TR and J7-TR cells (Figure 5a) but not when parental HepG2 and J7, or HepG2-Neo and J7-Neo cells were tested (Figure 5b). As Bcl-xL expression seemed to desensitize cancer cells to the apoptotic effect of TRAIL,<sup>16</sup> we hypothesized that Bcl-xL was one factor mediating the anti-apoptotic effect of  $T_3$ /TRs.

To explore the influence of Bcl-xL on TRAIL-mediated apoptosis of hepatoma cells, Bcl-xL expression in such cells was manipulated either by overexpression or shRNA-mediated knockdown. Overexpression of Bcl-xL caused dramatic reductions in the extent of TRAIL-induced apoptosis (Figures 5c-f). Simultaneously,  $T_3$  pretreatment protected control shRNA (sh-Luc)-transfected HepG2-TR and J7-TR

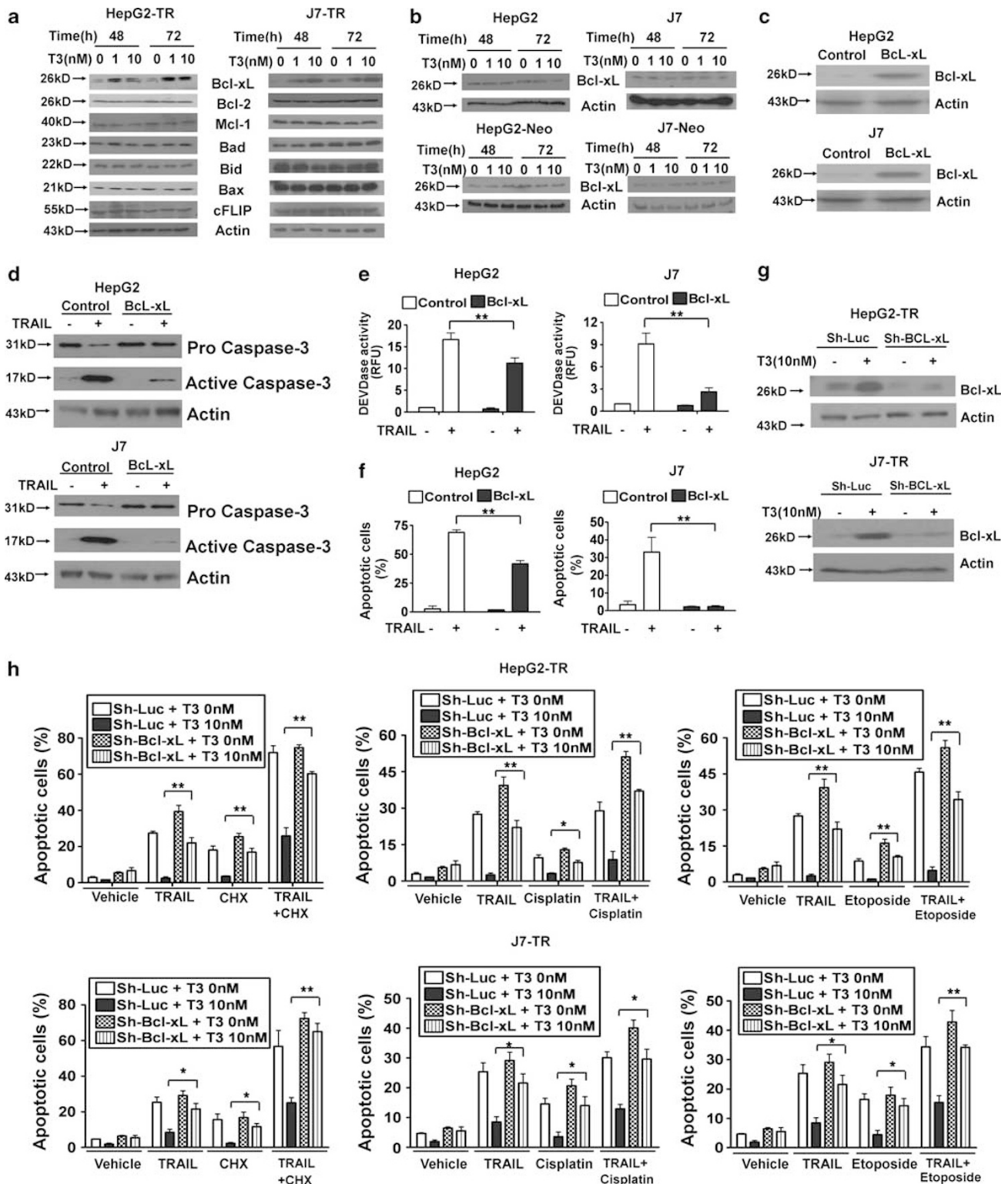
cells from apoptosis induced by r-TRAIL, chemotherapeutic drugs, or a combination of r-TRAIL and individual chemotherapeutic drugs. However, the anti-apoptotic effect of  $T_3$  was partially abolished in Bcl-xL-knockdown cells (Figures 5g, h; Supplementary Figure 9). These observations suggest that  $T_3$  simultaneously upregulates both *TRAIL* and anti-apoptotic factors such as *Bcl-xL*; the latter factor inhibits the apoptotic effects of TRAIL and chemotherapeutic drugs in TR-overexpressing hepatoma cells.

**TRAIL enhances the metastatic potential of apoptosis-resistant hepatoma cells.** Previous studies have shown that, apart from inducing apoptosis, TRAIL transduces non-apoptotic signals in tumor cells that are resistant to apoptosis. Among such signals, activation of NF- $\kappa$ B and MAPK are critical in the mediation of cell proliferation, differentiation, and migration.<sup>25</sup> We found that the NF- $\kappa$ B response reporter (Supplementary Figure 10A) or the level of activated p42/44 MAPK (phosphor-ERK 1/2; Supplementary Figure 10B) were dynamically activated by r-TRAIL. To further explore the non-apoptotic effects of TRAIL in hepatoma cells overexpressing Bcl-xL, we measured the expression levels of NF- $\kappa$ B and ERK target genes that promote migration and invasion in several types of cancer cells. We found that the expression levels of several members of the matrix metalloproteinase (MMP) family, including *MMP-2*, *MMP-9*, and *MMP-7*, were upregulated upon r-TRAIL stimulation of control HepG2 and J7; and HepG2-Bcl-xL and J7-Bcl-xL cells (Figure 6a). Interestingly, the induction of these genes was more prominent in Bcl-xL-overexpressing cells that were resistant to TRAIL-induced apoptosis. Similar activation patterns of these non-apoptotic target genes (evaluated at the protein level) were observed in r-TRAIL treated and adenovirus (Ad-TRAIL) infected HepG2-Bcl-xL and J7-Bcl-xL cells (Figure 6b; Supplementary Figure 11A). Moreover, gelatin zymography showed that MMP-2 and MMP-9 activities increased when TRAIL was expressed in HepG2-Bcl-xL and J7-Bcl-xL cells (Figure 6c; Supplementary Figure 11B). Together, these results imply that, although the pro-apoptotic function of TRAIL is inhibited by Bcl-xL, upregulation of TRAIL in hepatoma cells may facilitate cancer cell progression in other ways, perhaps by increasing the extent of invasion and metastasis. To further address this issue, a transwell assay was used to explore the metastatic capabilities of control and TRAIL-resistant Bcl-xL-overexpressing hepatoma cells subjected to TRAIL stimulation. After staining (with crystal violet) of cells that traversed the matrigel transwell membrane, we found that r-TRAIL or Ad-TRAIL induced invasion of HepG2-Bcl-xL and J7-Bcl-xL cells was significantly greater than was that of HepG2 and J7 control cells (Figure 6d; Supplementary Figure 11C). These gain-of-function studies revealed that TRAIL enhanced the metastatic potential of apoptosis-resistant hepatoma cells.

**$T_3$ -promoted hepatoma cell invasion is mediated by TRAIL.** The results discussed above suggested that upregulation of TRAIL by  $T_3$  in hepatoma cells triggered invasiveness of apoptosis-resistant cells, rather than inducing apoptosis. Whether  $T_3$ /TRs influenced hepatoma cell

metastasis required further examination. Upon transwell analysis, the invasive potential of control HepG2 and J7 cells was not changed upon addition of T<sub>3</sub> or a combination of T<sub>3</sub> with either control anti-IgG or the RIK-2 antibody (Supplementary Figure 12A). However, the invasive ability of

TR-overexpressing cells was significantly enhanced upon T<sub>3</sub> treatment, and addition of RIK-2 significantly reduced invasive cell numbers (Figure 7a). Additionally, RIK-2 partially suppressed the T<sub>3</sub>-induced expression of *MMP-2*, *-9*, and *-7* in TR-overexpressing hepatoma cells but not



in control hepatoma cells (Figure 7b; Supplementary Figure 12B). These results imply that T<sub>3</sub>-mediated upregulation of TRAIL promotes metastasis in TR-overexpressing hepatoma cells.

To explore whether T<sub>3</sub>/TRs-induced TRAIL expression and associated effects were evident *in vivo*, control IgG or RIK-2-

treated severe combined immunodeficiency (SCID) mice were injected with aliquots of 1 × 10<sup>7</sup> J7-TR cells, and next divided into euthyroid, hypothyroid, and hyperthyroid groups for 4 weeks before killing. Mice injected with J7-TR cells developed multiple macroscopic lung tumor nodules, as evidenced in hematoxylin and eosin (H&E)-stained sections.

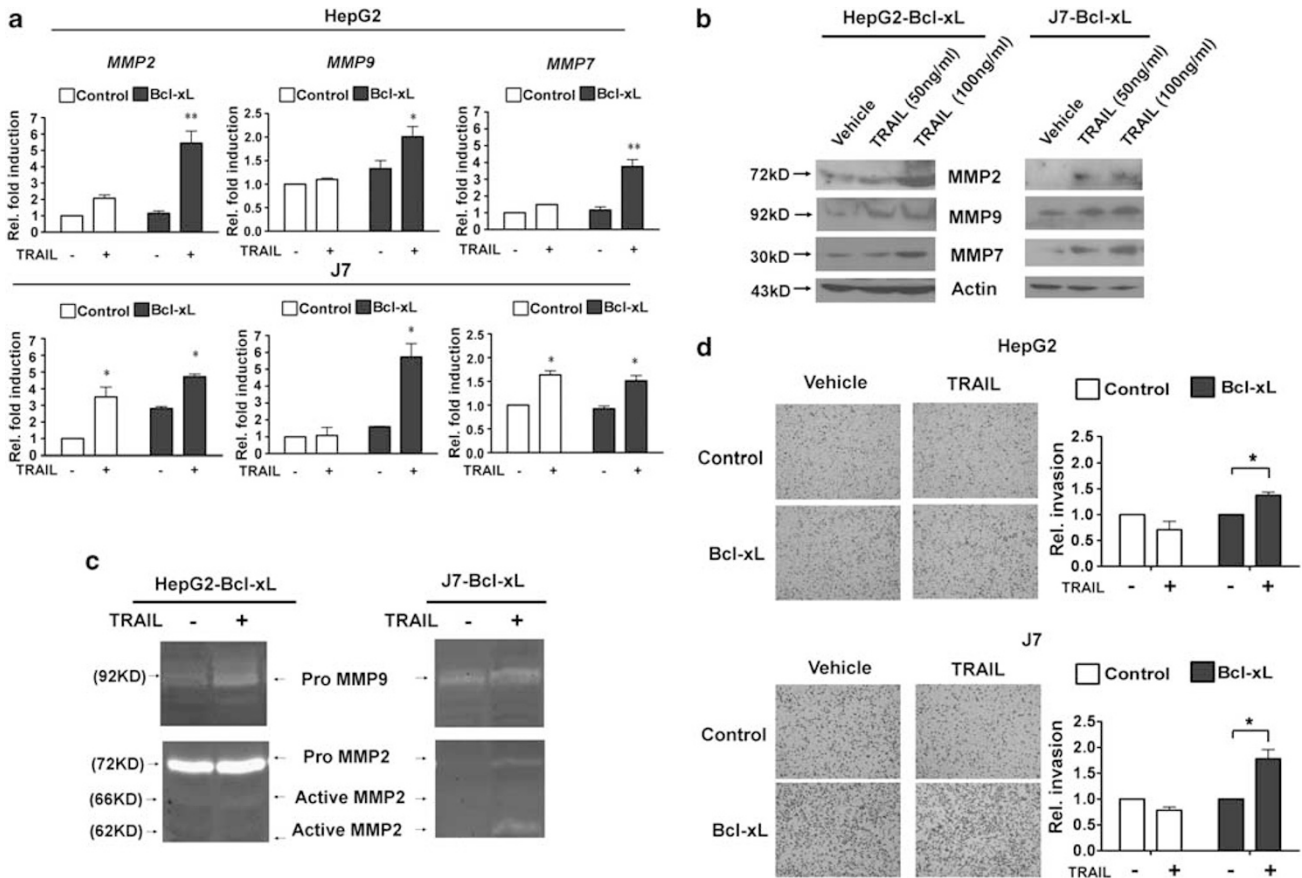


**Figure 6** TRAIL increases the metastatic potential of apoptosis-resistant hepatoma cells. (a) The expression levels of MMP-2, -7, and -9 in control or Bcl-xL-overexpressing hepatoma cell lines exposed to r-TRAIL for 24 h were measured using real-time PCR. The expression level in control cells (treated with vehicle only) was arbitrarily set to unity; the fold activation data presented are mean ± S.E.M. derived from the data of at least three experiments. Among-treatment differences were analyzed employing one-way ANOVA. \**P* < 0.05; \*\**P* < 0.01. (b) TRAIL induces expression of MMPs. After exposure to r-TRAIL for 48 h, conditioned media from HepG2-Bcl-xL and J7-Bcl-xL cells were analyzed by western blotting to detect MMPs. Actin served as an internal control. (c) Zymography revealing MMP-2 and -9 expression by HepG2-Bcl-xL and J7-Bcl-xL cells. Conditioned media from TRAIL-treated HepG2-Bcl-xL and J7-Bcl-xL cells were assayed for MMP activity as described in Materials and Methods. The electrophoretic positions of both the proenzymes and the active MMPs are shown. (d) TRAIL induces apoptosis-resistant cell invasion *in vitro*. HepG2-Py, J7-Py, HepG2-Bcl-xL, and J7-Bcl-xL cells (aliquots of 1 × 10<sup>5</sup> cells) were treated with r-TRAIL and placed in matrigel-coated wells. After incubation for 24 h at 37°C, cells that traversed the filters to attain the lower chambers were stained with crystal violet (left panels) and counted using microscopy. The proportion of traversed vehicle-treated control cells was arbitrarily set to unity and the relative fold proportions of traversing cells after exposure to various treatments are shown (right panels). All assays were repeated at least three times. Differences between data yielded by control and treated cells were evaluated using Student's *t*-test. \**P* < 0.05

**Figure 5** Bcl-xL overexpression suppresses TRAIL-induced apoptosis in hepatoma cells. (a) Expression of anti-apoptotic proteins in TR-overexpressing cells after T<sub>3</sub> treatment. HepG2-TR and J7-TR cells were cultured in Td medium for 24 h. Next, T<sub>3</sub> (1 or 10 nM) was added (or not) and growth continued for 48 or 72 h. Cell lysates (100 μg amounts) were subjected to western blotting using antibodies directed against Bcl-2, Bcl-xL, Mcl-1, Bad, Bid, Bax, cFLIP, or Actin. (b) Bcl-xL expression levels in HepG2, J7, HepG2-Neo, and J7-Neo cells treated (or not) with T<sub>3</sub> for 24 and 48 h were determined by western blotting. (c–e) Bcl-xL inhibits TRAIL-induced apoptosis in hepatoma cell lines. Bcl-xL was stably overexpressed in HepG2 and J7 cells and Bcl-xL levels in such cells were determined by western blotting (c). Next, these cell lines were stimulated with TRAIL (100 ng/ml) for 24 h and the extent of caspase-3 activation and the proportion of apoptotic cells were determined by western blotting (d), the DEVDase activity assay (e), and flow cytometry (f), respectively. (g and h) Bcl-xL knockdown suppresses the ability of T<sub>3</sub> to protect against apoptosis. HepG2 and J7 cells were stably transfected with sh-luc- or Bcl-xL-specific shRNAs and Bcl-xL levels in such cells were determined by western blotting (g). After stimulation with T<sub>3</sub> (0 or 10 nM) for 2 days, such stable lines were additionally stimulated with r-TRAIL (100 ng/ml), and/or chemotherapeutic drugs, individually or in combination, for 24 h, and the proportions of apoptotic cells and caspase-3 activity levels were determined using flow cytometry (h). The data are mean ± S.E.M. derived from experiments performed in triplicate; among-treatment differences were analyzed by one-way ANOVA. \**P* < 0.05; \*\**P* < 0.01



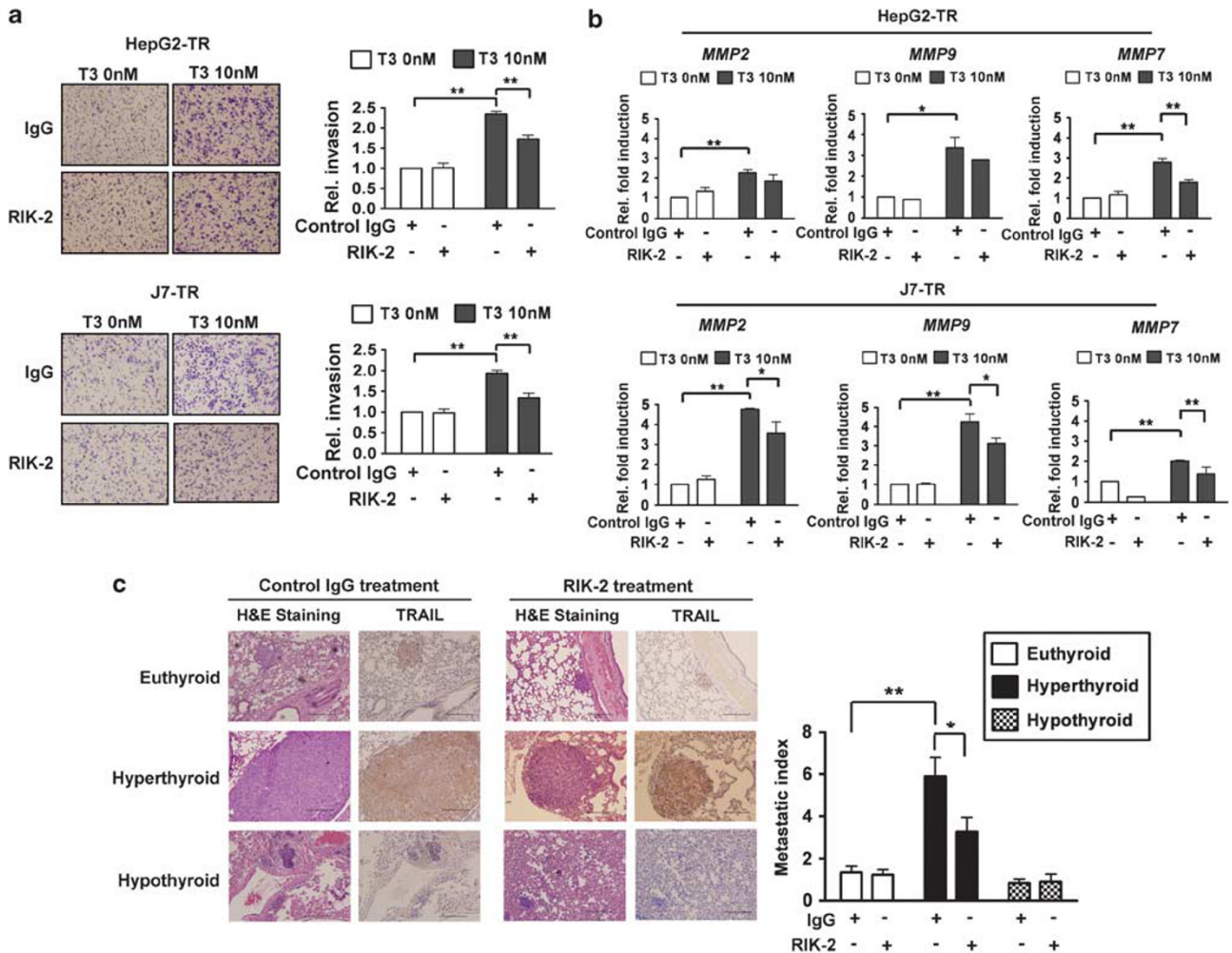


**Figure 7**  $T_3$ /TR-induced hepatoma cell metastasis is mediated by upregulation of TRAIL and MMPs. (a) The invasive properties of HepG2-TR and J7-TR cell lines treated (or not) with  $T_3$  (10 nM) in the presence of control IgG (10  $\mu$ g/ml) or RIK-2 (10  $\mu$ g/ml) were assessed as described above. Images of traversing cells (stained with crystal violet) are shown in the left panels and the relative proportions of cells that migrated to the lower chamber, compared with those of control IgG- and Td-treated cells, are shown in the right panels. All assays were repeated at least three times. Among-treatment differences were explored using one-way ANOVA. \* $P < 0.05$ ; \*\* $P < 0.01$ . (b) MMP synthesis is induced by  $T_3$ , but is partially blocked upon expression of RIK-2. The expression levels of *MMP-2*, *-7*, and *-9* in TR-overexpressing hepatoma cells, after  $T_3$ -induction, and upon exposure to control IgG or the RIK-2 antibody (10  $\mu$ g/ml) for 24 h, were evaluated using real-time PCR. The expression levels in cells treated with control IgG and Td were arbitrarily set to unity; the data presented are mean  $\pm$  S.E.M. of the results obtained in at least three experiments. Among-treatment differences were analyzed employing one-way ANOVA. \* $P < 0.05$ ; \*\* $P < 0.01$ . (c) Both  $T_3$ /TRs and TRAIL expression enhance hepatoma cell metastasis *in vivo*. Control SCID mice pretreated with IgG or RIK-2 received injections of  $1 \times 10^7$  J7-TR cells and were randomly divided into hypothyroid, euthyroid, and hyperthyroid groups ( $n = 6$  per group). All animals were sacrificed 4 weeks after cell injection and lungs were removed for tumor biopsy. H&E staining and TRAIL IHC images from lungs of the various mouse groups are shown in the left panels, respectively. Scale bar: 200  $\mu$ m. Metastatic indices (average fold increases in the density of tumor foci in hypothyroid, hyperthyroid, or euthyroid mice; per  $cm^2$  of lung area) are shown in the right panels

Although tumors developed in all groups, tumor numbers and sizes differed. Tumor size (relative to the average value) calculated per  $cm^2$  of lung section and the metastatic index were significantly greater in hyperthyroid mice than in euthyroid or hypothyroid animals. In addition, treatment with RIK-2 reduced  $\sim 35\%$  of the extent of lung metastasis in hyperthyroid mice (Figure 7c). The level of TRAIL expression (as evidenced by development of a dark-brown color upon immunohistochemical (IHC) staining) in metastatic lung tumors of hyperthyroid mice was markedly greater than in euthyroid and hypothyroid animals (Figure 7c). To validate the IHC results, a control IgG antibody was used in an effort to detect xenografts of either

GFP- or TRAIL-overexpressing J7-Bcl-xL cells in SCID mice; both tests were negative. Rather, an anti-TRAIL antibody yielded strong signals when used to stain TRAIL-overexpressing, but not GFP-overexpressing, J7-Bcl-xL xenografts (Supplementary Figure 13A).

**TRAIL is upregulated in human HCC tissue.** It was of interest to determine if  $T_3$ -induced TRAIL upregulation played an important role in HCC progression. To this end, IHC was employed to explore TRAIL expression levels in 65 HCC biopsy samples. We found that TRAIL was highly expressed in tumor cells, but staining of adjacent non-cancerous regions was relatively weak (Figures 8a and b).

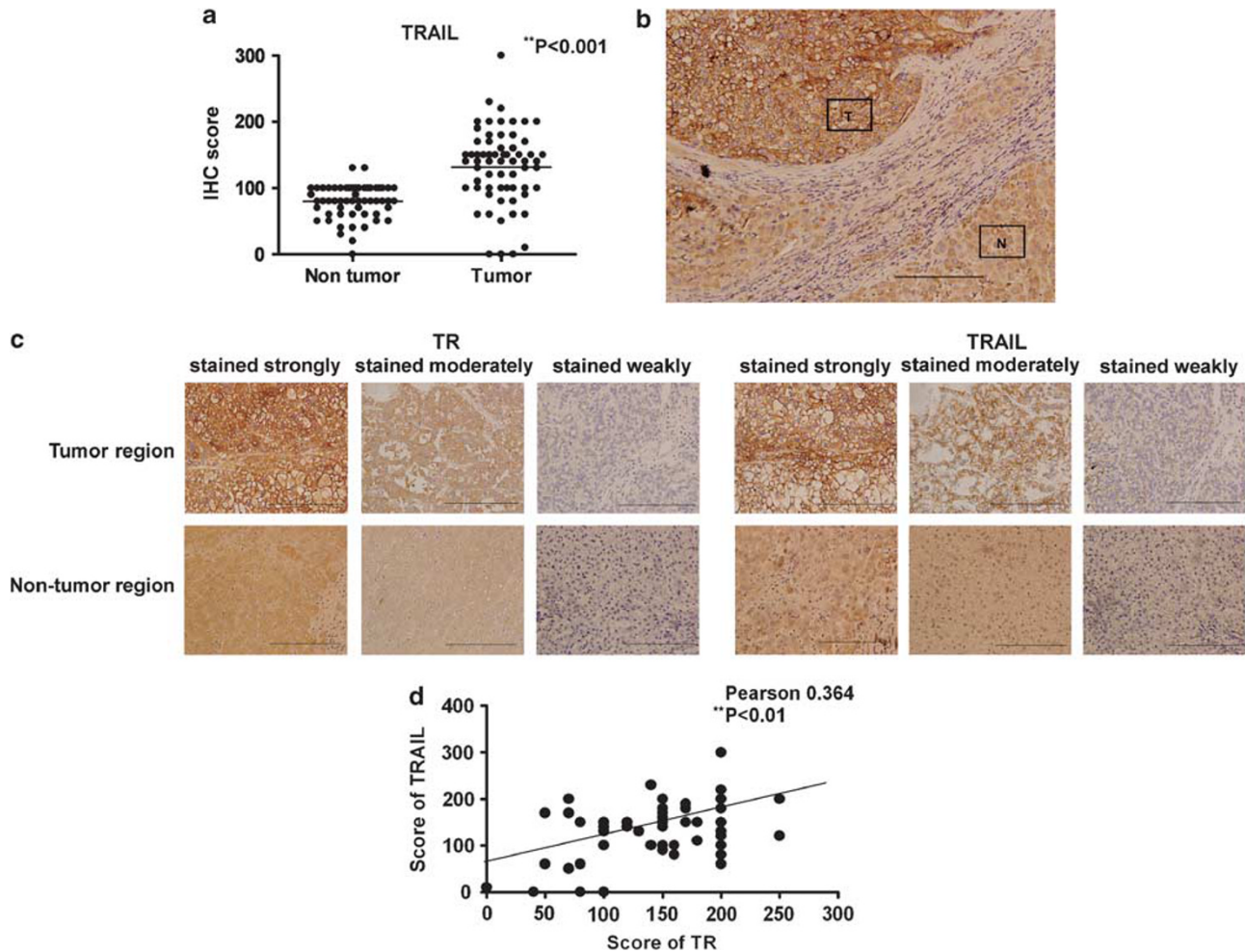


**Figure 8** TRAIL and TR expression levels are correlated in HCC tumors. Consecutive sections of 65 HCC biopsy samples were analyzed in terms of TRAIL and TR expression as described in Materials and Methods. The intensities of TRAIL expression in tumors, and adjacent non-cancerous regions, were scored, and the results are shown in (a), \*\* $P < 0.01$  by Student's  $t$ -test. (b) A representative image of an HCC specimen, including tumor (T) and adjacent non-tumor (N) cells, stained using a specific anti-TRAIL antibody ( $\times 200$ ). (c) Consecutive HCC tissue sections were incubated with anti-TR (left panel) and anti-TRAIL (right panel) antibodies before IHC. The samples were photographed ( $\times 400$ ) and antigen expression was scored as strong, moderate, or weak. (d) Correlation of TR and TRAIL expression levels in HCC tumors. Statistical significance was evaluated using the  $\chi^2$  test. \*\* $P < 0.01$

Of the 65 tumor specimens, 29 (45%) stained strongly, 25 (38%) stained moderately, and 11 (17%) stained weakly for TRAIL (Figure 8c). To further explore a possible correlation between TRAIL- and TR-expression levels in HCC tissues, consecutive tissue sections were subjected to IHC staining using an anti-TR antibody. Approximately 25 specimens (38%) exhibited strong staining for TR, 30 (46%) samples stained to a moderate extent and 10 (16%) stained weakly (Figure 8c). The data yielded by IHC staining of HCC sections for either TRAIL or TR were further verified by staining of such sections with control IgG; the staining patterns were uniformly negative (Supplementary Figure 13B). This showed that the anti-TR and anti-TRAIL antibodies were specific. Statistical analysis revealed that the TR-expression level was positively correlated with that of TRAIL (Figure 8d;  $r = 0.364$ ,  $P < 0.01$ ), strongly suggesting that TRAIL expression in HCC tumors is upregulated upon TR synthesis.

## Discussion

Circulating thyroid hormone and the cognate TR receptors, expressed in target tissues, have pivotal roles in regulating development and metabolic homeostasis in vertebrates. In addition, it is increasingly apparent that these materials have important roles in HCC. In the present study, we have highlighted a novel function of the  $T_3$ /TR complex in promoting the invasive ability of hepatoma cells. This function can be attributed to simultaneous upregulation of *TRAIL* and anti-apoptotic genes such as *Bcl-xL*. Induction of TRAIL by  $T_3$  enhances hepatoma cell invasion and expression of matrix metalloproteases, including MMP-2, -7, and -9. Importantly, IHC staining revealed that TRAIL expression increased in human liver cancers, compared with adjacent normal control tissue. Collectively, our findings show that TRs bind directly to the TRE of the *TRAIL* promoter to induce *TRAIL* transcription, which promotes metastasis rather than apoptosis because

*Bcl-xL* is simultaneously activated. This observation provides evidence for a new function of the increased TR and TRAIL levels evident in HCC.

T<sub>3</sub> and TRs have several roles in tumorigenesis. The use of genetic knockin mouse models has revealed that mutations in TR $\beta$  may lead to development of thyroid cancer and pituitary tumors. Moreover, the oncogenic activity of mutant TR $\beta$  is mediated by a combination of genomic and non-genomic mechanisms; gene expression and the activities of signaling pathways are subsequently affected.<sup>26</sup> Recently, Martinez-Iglesias *et al.*<sup>27</sup> reported that TRs serve as potent suppressors of tumor metastasis in hepatoma (SK-hep1) and breast cancer (MDA-MB-468) cells. The cited authors suggested that TR $\beta$ 1 expression in hepatoma and breast cancer cell lines, which have lost TR may retard tumor growth, trigger a partial mesenchyme-to-epithelium transition and suppress tumor metastasis in nude mice. Moreover, the data indicated that TRs might have diverse roles at different stages of tumorigenesis. The cited work showed that TR- $\alpha^{-/-}$  TR- $\beta^{-/-}$  double knockout mice were vulnerable to skin cancer, and that TR deficiency inhibited benign tumor formation at early stages but promoted malignant transformation at later stages of carcinogenesis.<sup>27</sup> However, the proposed tumor suppressor role of TRs remains controversial, with several investigators suggesting that TRs have an oncogenic function in tumorigenesis. For example, T<sub>3</sub> induces breast cancer cell and ovarian surface epithelial cell proliferation by influencing expression or activation of the estrogen receptor. Such data are supported by the epidemiological links that exist between hyperthyroidism and an increased risk of ovarian cancer.<sup>28,29</sup> Kress *et al.*,<sup>11</sup> using an animal model, found that TR $\alpha$ 1 directly regulated several components of the Wnt signaling pathway, facilitating the expression of  $\beta$ -catenin/Tcf4 target genes and promoting cell proliferation. Interestingly, overexpression of TR $\alpha$  in the intestinal epithelium did not induce cancer development, but rather accelerated tumorigenesis, in mice of a Wnt-activated Apc<sup>+/1638N</sup> genetic background. These diverse actions of TRs in carcinogenesis may be attributable to differences among various tissues and stages of specific tumor microenvironments.

TRAIL has been shown to induce apoptotic cell death in a wide variety of tumor cell lines *in vitro*, including hepatoma cells. Moreover, combination treatments with various chemotherapeutic agents (including CHX, cisplatin, or etoposide) sensitize tumor cells to TRAIL-induced apoptotic death.<sup>24</sup> However, in our experiments, T<sub>3</sub>-induced TRAIL expression did not cause the death of hepatoma cells. Conversely, in hepatoma cells challenged with chemotherapeutic drugs and TRAIL, T<sub>3</sub> displayed an anti-apoptotic effect, in a TR-dependent manner. Several anti-apoptotic signals or genes have been reported to suppress TRAIL-induced apoptosis.<sup>25</sup> Of these, Bcl-xL is of special interest, because the encoding gene is upregulated by T<sub>3</sub> in TR-overexpressing hepatoma cells. Previous studies showed that such overexpression reduced the extent of TRAIL-induced cell death in models of murine hepatitis and pancreatic ductal adenocarcinoma, whereas treatment with an inhibitor of Bcl-xL potentially enhanced TRAIL-triggered apoptosis of glioma cells.<sup>16,23,30</sup> Consistent with results obtained from the pancreatic ductal

adenocarcinoma studies, we found that Bcl-xL repressed TRAIL-triggered apoptosis of HepG2 and J7 cells. In addition to transmitting apoptotic signals, TRAIL stimulates non-apoptotic signaling. In human vascular endothelial cells, TRAIL enhances proliferation by activating the Akt and ERK pathways,<sup>31</sup> and promotes metastasis of tumor cells, including those of human pancreatic ductal adenocarcinoma, cholangiocarcinoma, and colorectal cancer, that are resistant to apoptotic death induced by NF- $\kappa$ B, Akt, or K-Ras activation.<sup>16–20</sup> Additionally, TRAIL induces chemotactic migration of monocytes by activation of the Rho-GTPase pathway<sup>32</sup> and has an important role in the immune escape of tumor cells. In colorectal cancers, effective apoptotic depletion of infiltrating CD8<sup>+</sup> immune cells is mediated by TRAIL.<sup>33,34</sup> These observations strongly suggest that TRAIL has oncogenic roles in apoptosis-resistant cancer cells. In our present study, cell invasion ability was significantly increased in HepG2-TR and J7-TR cells by the enhanced T<sub>3</sub> levels induced by TRAIL activation, as were the expression and activity levels of members of the matrix metalloprotease family, particularly MMP-2, -9, and -7. These proteins are key factors enhancing survival, invasion, and metastasis of several forms of malignant tumor cells.<sup>35–37</sup> In conclusion, our results show that cell invasion and metastasis are enhanced by non-apoptotic signals induced by TRAIL following T<sub>3</sub> treatment; apoptosis is not in play. We conclude that T<sub>3</sub> bound to TRs is a potent cancer promoter, particularly in a subset of HCC.

#### Materials and Methods

**Cell culture.** Hepatoma cell lines, including Huh7, the isogenic HepG2 and J7 cell lines, were routinely cultured in Dulbecco's Modified Eagle's Medium (DMEM) with 10% (v/v) FBS at 37 °C in a humidified atmosphere containing 5% (v/v) CO<sub>2</sub> and 95% (v/v) air. T<sub>3</sub>-depleted (Td) serum was prepared with the aid of AG 1-X8 resin (Bio-Rad, Hercules, CA, USA) and was added to DMEM at 10% (v/v) to form Td medium. T<sub>3</sub> was purchased from Sigma-Aldrich (St. Louis, MO, USA).

**Real-time PCR.** Hepatoma cells were seeded into 10 cm diameter dishes and exposed to various treatments for the indicated times before harvesting for RNA extraction. Total RNA was purified using the TRIzol reagent (Life Technologies Inc., Carlsbad, CA, USA) according to the supplier's protocol, and cDNA was next synthesized using a Superscript II kit (Life Technologies, Karlsruhe, Germany). Real-time PCR was conducted in 15  $\mu$ l reaction mixtures containing 25 nM of forward and reverse primers, and 1  $\times$  SYBR Green reaction mix (Applied Biosystems, Carlsbad, CA, USA). All reactions were conducted in an ABI PRISM 7500 sequencer (Applied Biosystems, Foster City, CA, USA).

**Immunoblotting.** Total cell lysates and conditioned media were analyzed using 12% (w/v) SDS-PAGE, separated proteins were transferred to PVDF membranes. After several washes in PBST (PBS containing 0.05% (v/v) Tween 20), blots were incubated in blocking solution (PBST with 5% (w/v) skim milk powder) containing a primary antibody at room temperature for 2 h. Next, an HRP-conjugated secondary antibody, dissolved in blocking solution, was added (after thorough washing of blots). Signals were detected via the chemiluminescence elicited using an ECL kit (Amersham Inc., Piscataway, NJ, USA) and were recorded on X-ray film. A rabbit polyclonal antibody directed against human TRAIL was purchased from AbD Serotec (Oxford, UK). Rabbit anti-human antibodies directed against Bcl-xL, Bcl-2, Mcl-1, Bad, Bid, Bax, pro-caspase-3, pro-caspase-8, active caspase-3, and cFLIP were purchased from Epitomics (Burlingame, CA, USA). A mouse anti-human fascin monoclonal antibody was the product of Santa Cruz Biotechnology (Santa Cruz, CA, USA). Rabbit antibodies directed against ERK1/2, phospho-ERK1/2, and active caspase-8 were obtained from Cell Signaling Technology (Boston, MA, USA). Image data were quantified using 'Image-gauge' software (Fujifilm, Tokyo, Japan). The expression levels of TRAIL in

cells treated with vehicle only were arbitrarily set to unity. Next, the relative levels of *TRAIL* expression in cells induced by  $T_3$  (10 nM) were calculated.

**Transient transfection and reporter assays.** The 5'-flanking region (-3899 to +30 bp) of the *TRAIL* gene was amplified from genomic DNA using PCR and inserted into the pGL3-basic vector to generate a P1 reporter construct. Three 5'-deletions (P3, P4, and P7) and two TRE mutants (P5 and P6) derived from this reporter were generated by PCR amplification and inserted between the same sites of pGL3-basic. To explore the response to  $T_3$  addition, HepG2-TR cells were transfected with 0.2  $\mu$ g of each *TRAIL* promoter-driven reporter construct and 0.05  $\mu$ g of the SV $\beta$  vector (Clontech, Palo Alto, CA, USA), expressing  $\beta$ -galactosidase, for 16 h. Next, cells were treated with  $T_3$  (0, 10, or 100 nM) and incubated for 24 h before harvesting; luciferase and  $\beta$ -galactosidase activities were subsequently measured. Luciferase activity was normalized to that of  $\beta$ -galactosidase.

**ChIP assay.** DNA and protein of HepG2-TR $\alpha$  cells were cross-linked by addition of 1% (v/v) formaldehyde to the culture medium, for 10 min at room temperature. The reaction was next terminated by the addition of 0.125 M glycine. After washing with ice-cold PBS, cells were resuspended in RIPA buffer (50 mM Tris, pH 8.0, with 0.1% (w/v) sodium deoxycholate, 0.1% (w/v) SDS, 150 mM NaCl, and 5 mM EDTA) containing protease inhibitors (1 mM of each of PMSF, aprotinin, and leupeptin). Next, the suspensions were sonicated (to shear chromatin) using a Misonix Sonicator 3000 Homogenizer (Mandel Scientific Company Inc., Guelph, ON, Canada). The sheared DNA fragments were in the size range 0.1–1 kb. All samples were next precleared by the addition of 60  $\mu$ l amounts of protein A/G-agarose (Sigma-Aldrich) for 30 min at 4 °C. Next, an anti-TR antibody (the kind gift of Dr. S-Y Cheng) or an anti-IgG antibody (R&D Systems, Minneapolis, MN, USA) was added and incubation proceeded at 4 °C overnight before the addition of 80  $\mu$ l of a protein A/G-agarose suspension (to pull down any relevant DNA/protein complex). A 186-bp fragment of the *TRAIL* promoter containing the predicted TRE was detected by PCR using the forward primer 5'-GAGATGGAGTTTCACCGTGTAGC-3' and reverse primer 5'-AGAGTGTGGAATAAGGAGGCTTA-3'. The TRE region of the *Furin* promoter was amplified using the forward primer 5'-TACTAGCGTTTTACGGGCG-3' and reverse primer 5'-TCGAACAGGAGCAGAGAGCGA-3'; this served as a positive control for amplification of the TR-targeting site. A 166-bp fragment of *Gapdh*, lacking a TRE, was detected using the forward primer 5'-CTCAAAGACCCACTGCG-3' and reverse primer 5'-CCACTTGTCTCAGGCCTAG-3'; this served as a negative control.

**Assay of DEVDase and IETDase proteolytic activities.** The levels of caspase-3 and -8 were determined using the 7-amino-4-trifluoromethyl coumarin assay (AFC) that employs the tetrapeptides DEVD (a synthetic caspase 3 substrate) and IETD (a synthetic caspase 8 substrate), as recommended by the manufacturer (BioVision, Mountain View, CA, USA). After stimulation with an apoptotic agent, caspases activated in apoptotic cells cleave synthetic substrates to release free AFC, which is next quantified by fluorometry. In each reaction, a 200- $\mu$ g amount of cell lysate in 100  $\mu$ l reaction buffer containing 5 mM DTT was incubated with 50 mM DEVD-AFC or IETD-AFC at 37 °C for 120 min. Finally, reaction outcomes were analyzed by fluorometry (SpectraMax M2, Molecular Device, Sunnyvale, CA, USA) employing a 400-nm excitation filter and a 505-nm emission filter. The fluorescence intensity was proportional to caspase activity.

**Assay of apoptosis by flow cytometry.** Parental or derived stable hepatoma cell lines were treated with chemotherapeutic drugs, or r-*TRAIL*, after exposure to  $T_3$  (0 or 10 nM) for 48 h. Cells were harvested via trypsinization and washed with complete cell culture medium (to terminate tryptic digestion) before collection (using centrifugation at  $300 \times g$  for 5 min). Next, the cells were fixed in ethanol/PBS (7:3, v/v) for 1 h at -20 °C. After fixation, cells were pelleted by centrifugation and resuspended in PBS containing 40  $\mu$ g/ml RNase A and 0.5% (v/v) Triton X-100 for 1 h at 37 °C. Finally, the cells were pelleted once more and resuspended in PBS containing 50  $\mu$ g/ml propidium iodide (Sigma). The extent of genomic DNA fragmentation was quantified using flow cytometric analysis of hypodiploid DNA. Data were collected and analyzed using FACSscan (Becton Dickinson, San Jose, CA, USA) running CellQuest software.

**Zymography.** Concentrated medium (containing 80  $\mu$ g amounts of protein) was diluted in 50 mM Tris-HCl (pH 7.4) in the absence of any reducing agent,

and proteins were separated on 8% (w/v) SDS-PAGE gels containing 1 mg/ml gelatin. After electrophoresis, each gel was washed twice in 2.5% (v/v) Triton X-100 (in 50 mM Tris-HCl, pH 7.4) for 15 min and next incubated for 16 h at 37 °C in developing buffer (10 mM  $CaCl_2$ , 150 mM NaCl, and 0.02% (w/v)  $Na_2S_2O_5$  in 50 mM Tris-HCl (pH 7.5)). Gels were stained with Coomassie Blue and destained until clear bands appeared.

**In vitro invasion assay.** The influence of  $T_3$  on the *TRAIL*-mediated invasive activity of TR-overexpressing hepatoma cell lines was assessed using the rapid transwell *in vitro* assay. Cell density was adjusted to  $1 \times 10^5$  cells/ml, and a 1-ml volume of cell suspension was added to each upper chamber coated with Matrigel (Becton-Dickinson, Franklin Lakes, NJ, USA); all tests were performed in triplicate. Serum-free DMEM was added to the upper chamber, whereas the lower chamber contained DMEM supplemented with 20% (v/v) FBS. After incubation for 24 h at 37 °C, cells traversing the filter, to attain the lower chamber, were stained with crystal violet and counted.

**Xenograft models of tumor progression and metastasis.** To investigate  $T_3$ -induced *TRAIL* expression *in vivo* and its physiological consequences, SCID mice were intraperitoneally injected with 100  $\mu$ g amounts of control IgG or the RIK-2 antibody once every 3 days, commencing 3 days before tumor inoculation. After tail vein injection of  $1 \times 10^7$  J7-TR tumor cells, control IgG- or RIK-2-treated mice were divided into three groups, each containing six animals. Euthyroid animals received vehicle (PBS) in drinking water for 4 weeks. After being killed, serum was collected for analysis of  $T_3$  and TSH levels. The serum  $T_3$  level in hypothyroid mice (15.87 ng/dl) was approximately 0.025-fold to that in  $T_3$ -treated animals (619 ng/dl). However, the serum TSH levels in hypothyroid and hyperthyroid mice were 86.368 and 0.008  $\mu$ U/ml, respectively. The serum  $T_3$  and TSH levels of euthyroid mice were about 45.5 ng/dl and 0.246  $\mu$ U/ml, respectively. To induce hypothyroidism in SCID mice, methimazole (0.2 g/l) and sodium perchlorate (1 g/l) were added to drinking water after inoculation of tumor cells. Hyperthyroid mice were generated by addition of  $T_3$  (2.5 mg/l) to drinking water after injection of tumor cells. All animals were killed 4 weeks after tumor inoculation, and livers and lungs were removed for tumor biopsy. Formalin-fixed paraffin-embedded tissues were examined by H&E staining, and employing IHC and a specific anti-*TRAIL* antibody. *TRAIL* immunoreactivity was evidenced by the development of a dark brown color. All procedures followed the United States National Institutes of Health guidelines and the Guide for the Care and Use of Laboratory Animals issued by the Chang-Gung Institutional Animal Care and Use Committee.

**Human HCC specimens.** Biopsies of 65 patients diagnosed with HCC were selected for study after informed consent was obtained from all patients. All HCC tissue samples, paired with adjacent non-tumor liver tissue specimens, were obtained by the Chang Gung Memorial Hospital Medical Research Center and were subjected to IHC analysis. HCC and adjacent non-cancerous liver tissue samples were examined by H&E staining. Our study protocol was approved by the Medical Ethics and Human Clinical Trial Committee of the Chang-Gung Memorial Hospital.

**Immunohistochemical staining.** IHC analyses were performed automatically using a Bond-max Automated Immunostainer (Vision Biosystems, Melbourne, VIC, Australia). Consecutive tissue sections were retrieved using Bond Epitope Retrieval Solution 1 (Vision BioSystems) and stained with either a rabbit polyclonal antibody directed against *TRAIL* or a mouse monoclonal antibody against TR. A polymer detection system (Bond Polymer Refine; Vision BioSystems) was used to reduce non-specific noise. Subsequently, sections were treated with DAB buffer containing the chromogen 3,3'-diaminobenzidine and next counterstained with hematoxylin. TR- and *TRAIL*-positive tumor cells in representative microscopic fields were independently scored by two pathologists (YL and SMJ) blinded to all clinical data. Staining was graded as absent (0), weak (1+), medium (2+), or strong (3+). A histoscore (*H*) was calculated by multiplying the percentages (*Ps*) of positive cells by the staining intensities (*I*) as previously described.<sup>38</sup> Thus,  $H = \sum [P \times I]$ .

**Statistical analysis.** All results are mean  $\pm$  S.E.M. of data derived in at least three independent experiments. Statistical analysis was performed using Student's *t*-test or one-way ANOVA, as indicated in the figure legends.

**Conflict of Interest**

The authors declare no conflict of interest.

**Acknowledgements.** This work was supported by grants from Chang-Gung University, Taoyuan, Taiwan (CMRPD 34013, NMRP 140511) and National Science Council of the Republic of China (NSC 94–2320-B-182–052).

- Huang YH, Tsai MM, Lin KH. Thyroid hormone dependent regulation of target genes and their physiological significance. *Chang Gung Med J* 2008; **31**: 325–334.
- Gonzalez-Sancho JM, Garcia V, Bonilla F, Munoz A. Thyroid hormone receptors/THRs genes in human cancer. *Cancer Lett* 2003; **192**: 121–132.
- Barlow C, Meister B, Lardelli M, Lendahl U, Vennstrom B. Thyroid abnormalities and hepatocellular carcinoma in mice transgenic for v-erbA. *Embo J* 1994; **13**: 4241–4250.
- Sap J, Munoz A, Damm K, Goldberg Y, Ghysdael J, Leutz A *et al*. The c-erb-A protein is a high-affinity receptor for thyroid hormone. *Nature* 1986; **324**: 635–640.
- Lin KH, Shieh HY, Chen SL, Hsu HC. Expression of mutant thyroid hormone nuclear receptors in human hepatocellular carcinoma cells. *Mol Carcinog* 1999; **26**: 53–61.
- Chan IH, Privalsky ML. Thyroid hormone receptors mutated in liver cancer function as distorted antimorphs. *Oncogene* 2006; **25**: 3576–3588.
- Chan IH, Privalsky ML. Thyroid hormone receptor mutants implicated in human hepatocellular carcinoma display an altered target gene repertoire. *Oncogene* 2009; **28**: 4162–4174.
- Davis FB, Tang HY, Shih A, Keating T, Lansing L, Hercberts A *et al*. Acting via a cell surface receptor, thyroid hormone is a growth factor for glioma cells. *Cancer Res* 2006; **66**: 7270–7275.
- Plateroti M, Kress E, Mori JI, Samarut J. Thyroid hormone receptor alpha1 directly controls transcription of the beta-catenin gene in intestinal epithelial cells. *Mol Cell Biol* 2006; **26**: 3204–3214.
- Wu SM, Huang YH, Yeh CT, Tsai MM, Liao CH, Cheng WL *et al*. Cathepsin H regulated by the thyroid hormone receptors associate with tumor invasion in human hepatoma cells. *Oncogene* 2011; **30**: 2057–2069.
- Kress E, Skah S, Sirakov M, Nadjar J, Gadot N, Scoazec JY *et al*. Cooperation between the thyroid hormone receptor TR $\alpha$ 1 and the WNT pathway in the induction of intestinal tumorigenesis. *Gastroenterology* 2010; **138**: 1863–1874; e1.
- Ishii H, Tatsuta M, Baba M, Okuda S, Taniguchi H. Enhancement by thyroxine of experimental carcinogenesis induced in rat colon by azoxymethane. *Int J Cancer* 1992; **50**: 974–976.
- Wiley SR, Schooley K, Smolak PJ, Din WS, Huang CP, Nicholl JK *et al*. Identification and characterization of a new member of the TNF family that induces apoptosis. *Immunity* 1995; **3**: 673–682.
- Pitti RM, Marsters SA, Ruppert S, Donahue CJ, Moore A, Ashkenazi A. Induction of apoptosis by Apo-2 ligand, a new member of the tumor necrosis factor cytokine family. *J Biol Chem* 1996; **271**: 12687–12690.
- Johnstone RW, Frew AJ, Smyth MJ. The TRAIL apoptotic pathway in cancer onset, progression and therapy. *Nat Rev Cancer* 2008; **8**: 782–798.
- Trauzold A, Siegmund D, Schniewind B, Sipsos B, Egberts J, Zorenkov D *et al*. TRAIL promotes metastasis of human pancreatic ductal adenocarcinoma. *Oncogene* 2006; **25**: 7434–7439.
- Ehrenschwender M, Siegmund D, Wicovsky A, Kracht M, Dittrich-Breiholz O, Spindler V *et al*. Mutant PIK3CA licenses TRAIL and CD95L to induce non-apoptotic caspase-8-mediated ROCK activation. *Cell Death Differ* 2010; **17**: 1435–1447.
- Ishimura N, Isomoto H, Bronk SF, Gores GJ. Trail induces cell migration and invasion in apoptosis-resistant cholangiocarcinoma cells. *Am J Physiol Gastrointest Liver Physiol* 2006; **290**: G129–G136.
- Hoogwater FJ, Nijkamp MW, Smakman N, Steller EJ, Emmink BL, Westendorp BF *et al*. Oncogenic K-Ras turns death receptors into metastasis-promoting receptors in human and mouse colorectal cancer cells. *Gastroenterology* 2010; **138**: 2357–2367.
- Fingas CD, Blechacz BRA, Smoot RL, Guicciardi ME, Mott J, Bronk SF *et al*. A smac mimetic reduces TNF related apoptosis inducing ligand (TRAIL)-induced invasion and metastasis of cholangiocarcinoma cells. *Hepatology* 2010; **52**: 550–561.
- Spierings DC, de Vries EG, Timens W, Groen HJ, Boezen HM, de Jong S. Expression of TRAIL and TRAIL death receptors in stage III non-small cell lung cancer tumors. *Clin Cancer Res* 2003; **9**: 3397–3405.
- Ozawa F, Friess H, Kleeff J, Xu ZW, Zimmermann A, Sheikh MS *et al*. Effects and expression of TRAIL and its apoptosis-promoting receptors in human pancreatic cancer. *Cancer Lett* 2001; **163**: 71–81.
- Zender L, Hutker S, Mundt B, Waltemathe M, Klein C, Trautwein C *et al*. NF $\kappa$ B-mediated upregulation of bcl-xl restrains TRAIL-mediated apoptosis in murine viral hepatitis. *Hepatology* 2005; **41**: 280–288.
- Muhlethaler-Mottet A, Bourlout KB, Auderset K, Joseph JM, Gross N. Drug-mediated sensitization to TRAIL-induced apoptosis in caspase-8-complemented neuroblastoma cells proceeds via activation of intrinsic and extrinsic pathways and caspase-dependent cleavage of XIAP, Bcl-xL and RIP. *Oncogene* 2004; **23**: 5415–5425.
- Malhi H, Gores GJ. TRAIL resistance results in cancer progression: a TRAIL to perdition? *Oncogene* 2006; **25**: 7333–7335.
- Guigon CJ, Cheng SY. Novel oncogenic actions of TRbeta mutants in tumorigenesis. *IUBMB Life* 2009; **61**: 528–536.
- Martinez-Iglesias O, Garcia-Silva S, Tenbaum SP, Regadera J, Larcher F, Paramio JM *et al*. Thyroid hormone receptor beta1 acts as a potent suppressor of tumor invasiveness and metastasis. *Cancer Res* 2009; **69**: 501–509.
- Hall LC, Salazar EP, Kane SR, Liu N. Effects of thyroid hormones on human breast cancer cell proliferation. *J Steroid Biochem Mol Biol* 2008; **109**: 57–66.
- Rae MT, Gubbay O, Kostogiannou A, Price D, Critchley HO, Hillier SG. Thyroid hormone signaling in human ovarian surface epithelial cells. *J Clin Endocrinol Metab* 2007; **92**: 322–327.
- Hetschko H, Voss V, Horn S, Seifert V, Prehn JH, Kogel D. Pharmacological inhibition of Bcl-2 family members reactivates TRAIL-induced apoptosis in malignant glioma. *J Neurooncol* 2008; **86**: 265–272.
- Secchiero P. TRAIL promotes the survival and proliferation of primary human vascular endothelial cells by activating the Akt and ERK pathways. *Circulation* 2003; **107**: 2250–2256.
- Wei W, Wang D, Shi J, Xiang Y, Zhang Y, Liu S *et al*. Tumor necrosis factor (TNF)-related apoptosis-inducing ligand (TRAIL) induces chemotactic migration of monocytes via a death receptor 4-mediated RhoGTPase pathway. *Mol Immunol* 2010; **47**: 2475–2484.
- Grimm M, Kim M, Rosenwald A, von Rahden B, Tsaui I, Meier E *et al*. Tumour-mediated TRAIL-receptor expression indicates effective apoptotic depletion of infiltrating CD8 + immune cells in clinical colorectal cancer. *Eur J Cancer* 2010; **46**: 2314–2323.
- Huber V, Fais S, Iero M, Lugini L, Canese P, Squarcina P *et al*. Human colorectal cancer cells induce T-cell death through release of proapoptotic microvesicles: role in immune escape. *Gastroenterology* 2005; **128**: 1796–1804.
- Zhou DH, Trauzold A, Roder C, Pan G, Zheng C, Kalthoff H. The potential molecular mechanism of overexpression of uPA, IL-8, MMP-7 and MMP-9 induced by TRAIL in pancreatic cancer cell. *Hepatobiliary Pancreat Dis Int* 2008; **7**: 201–209.
- Sternlicht MD, Werb Z. How matrix metalloproteinases regulate cell behavior. *Annu Rev Cell Dev Biol* 2001; **17**: 463–516.
- Kim JH, Choi C, Benveniste EN, Kwon D. TRAIL induces MMP-9 expression via ERK activation in human astrocytoma cells. *Biochem Biophys Res Commun* 2008; **377**: 195–199.
- Liao CJ, Wu TI, Huang YH, Chang TC, Wang CS, Tsai MM *et al*. Glucose-regulated protein 58 modulates cell invasiveness and serves as a prognostic marker for cervical cancer. *Cancer Sci* 2011; **102**: 2255–2263.

Supplementary Information accompanies the paper on Cell Death and Differentiation website (<http://www.nature.com/cdd>)